Catalysis Today 176 (2011) 409–412

Contents lists available at ScienceDirect

Catalysis Today

journal homepage: www.elsevier.com/locate/cattod

The role of alumina support in the deoxygenation of rapeseed oil over NiMo–alumina catalysts

Peter Priecel[a], Libor Čapek[a,*], David Kubička[b], František Homola[b], Petr Ryšánek[b], Miloslav Pouzar[a]

[a] Faculty of Chemical Technology, University of Pardubice, Studentská 573, 532 10 Pardubice, Czech Republic
[b] Department of Refinery and Petrochemical Research, Research Institute of Inorganic Chemistry, Záluží 1, 436 70 Litvínov, Czech Republic

ARTICLE INFO

Article history:
Received 19 September 2010
Received in revised form 4 November 2010
Accepted 5 November 2010
Available online 16 December 2010

Keywords:
Deoxygenation
NiMo–alumina
UV–vis
Mesoporous alumina

ABSTRACT

Deoxygenation of rapeseed oil was studied over NiMo–alumina catalysts. The research was focused on supporting of Ni and Mo species on a conventional alumina (255 $m^2 g^{-1}$) and a commercially available mesoporous alumina (520 $m^2 g^{-1}$) supports and on establishing their catalytic performance. The NiMo–alumina/meso catalyst showed significantly better performance than the NiMo–alumina catalyst in deoxygenation of rapeseed oil. The better performance was attributed to the significantly higher specific surface area and the total pore volume of NiMo–alumina/meso in comparison with the NiMo–alumina.

© 2010 Elsevier B.V. All rights reserved.

1. Introduction

Transesterification, thermal and catalytic cracking and deoxygenation have been developed to produce the renewable fuels from vegetable oils [1]. In general, the term deoxygenation can refer to several reactions, mainly decarboxylation, decarbonylation, dehydration and hydrodeoxygenation, and is often accompanied by hydrogenation of double bonds [1,2]. The advantage of deoxygenation over transesterification and cracking is that it yields straight-chain alkanes having 15–20 carbon atoms, which, after isomerisation, are much alike the hydrocarbons found in conventional diesel. Different types of catalysts have been investigated in deoxygenation reactions with particular focus on CoMo–alumina [3], NiMo–alumina [4–6] and NiMoP–alumina [5] catalysts.

It is generally accepted that mesoporous materials offer a great potential as support for the active species in the catalytic processes [7,8]. Mesoporous alumina supports offer several advantages over conventional alumina supports, such as high specific surface area resulting in a possibility to achieve high dispersion and loading of active species on the support and narrow pore size distribution with pore size ranging from 2 to more than 10 nm [7] enabling the access of large organic molecules to the active sites situated inside the pores.

Previously, Kubička et al. [9] showed high potential of CoMo species supported on the organized mesoporous materials synthesized in a laboratory. In the present work, the attention is focused on supporting of Ni and Mo species on commercially available mesoporous and conventional alumina supports and the comparison of the activity/selectivity of NiMo–alumina/meso and NiMo–alumina catalysts in the deoxygenation of rapeseed oil.

2. Experimental

Alumina (denoted as alumina, 255 $m^2 g^{-1}$) and mesoporous alumina (denoted as alumina/meso, 520 $m^2 g^{-1}$) were supplied by Eurosupport Manufacturing Czechia and NanoScale Corporation, respectively. NiMo–alumina catalysts were prepared by impregnating the alumina supports with an ethanol solution of nickel acetonate tetrahydrate and molybdenyl acetylacetonate followed by calcination at 600 °C in the air flow for 5 h. NiMo–alumina and NiMo–alumina/meso catalysts were prepared with the same amount of Ni (3.0 wt.%) and Mo (6.0 wt.%). The concentration of the Ni and Mo species in the catalysts was determined with Elvatech desktop energy-dispersive XRF spectrometer Elva X equipped with a Ti anode X-ray tube. X-ray diffractograms were recorded with Bruker AXE D8-Advance diffractometer using Cu Kα radiation with a secondary graphite monochromator. UV–vis diffuse reflectance spectra of granulated catalysts (particle size 0.25–0.50 mm) were recorded using GBC CINTRA 303 spectrometer equipped with a spectralon-coated integrating sphere against a spectralon reference. The specific surface areas and the pore size distributions of the catalysts were obtained by Coulter SA 3100 Surface Area and

* Corresponding author.
E-mail addresses: libor.capek@upce.cz (L. Čapek), david.kubicka@vuanch.cz (D. Kubička).

0920-5861/$ – see front matter © 2010 Elsevier B.V. All rights reserved.
doi:10.1016/j.cattod.2010.11.022

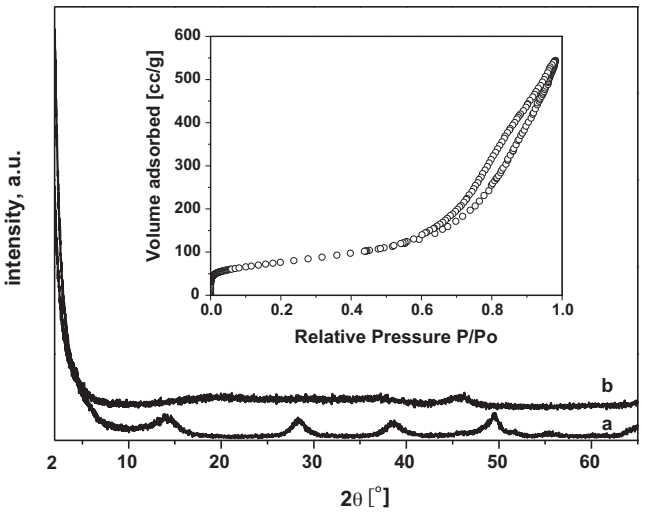

Fig. 1. (A) XRD patterns of alumina–meso (a) and NiMo–alumina–meso materials (b) and (B) adsorption/desorption isotherms of NiMo–alumina–meso catalyst.

Pore Size Analyzer. Specific surface area was calculated by the BET method and the pore size distribution (pore diameter and pore volume) was determined by the BJH method. Deoxygenation of rapeseed oil was performed in a bench-scale fixed-bed reactor of 17 mm inner diameter. Firstly, catalysts were mixed with silicon carbide and sulfided with 5 vol.% dimethyl disulfide in iso-octane at 340 °C. Secondly, the deoxygenation of rapeseed oil was studied under hydrogen (3.5 MPa and H2/rapeseed oil molar ratio 50) at 260–280 °C and *W/F* 0.25–1 h^{-1} [9].

3. Results and discussion

The specific surface area of conventional alumina support was 255 $m^2\ g^{-1}$, while the specific surface area of alumina/meso was 520 $m^2\ g^{-1}$. The mesoporous alumina structure of alumina/meso material was confirmed by XRD (Fig. 1) and sorption isotherm of nitrogen. The diffraction pattern of alumina/meso (Fig. 1) showed the intensive diffraction peak at 2–3°, typical for organized mesoporous aluminas [7]. Nevertheless, it should be mentioned that the low angle diffraction peak corresponds to the mesopores with high pores diameter and long distance atom ordering [10].

Fig. 2 shows the pore size distribution and the physicochemical properties of the NiMo–alumina and NiMo–alumina/meso catalysts. NiMo–alumina/meso catalyst exhibited a broad pore size distribution (Fig. 2B) owing to the commercially available mesoporous alumina properties. On the other hand, the pore size distribution of mesoporous alumina materials synthesized at lab was reported to have narrow pore size distribution [7]. The specific surface area of NiMo–alumina/meso (273 $m^2\ g^{-1}$) was significantly higher in comparison with NiMo–alumina catalyst (193 $m^2\ g^{-1}$). The decrease in the specific surface area was higher after the impregnation of Ni and Mo species on the alumina/meso support (48%) in comparison with the impregnation of Ni and Mo species on alumina support (25%). Addition of Ni and Mo species on the alumina/meso support decreased the specific surface area (from 520 $m^2\ g^{-1}$ to 272 $m^2\ g^{-1}$) and total pore volume (from 1.3032 $cm^3\ g^{-1}$ to 0.8402 $cm^3\ g^{-1}$) suggesting that the impregnated Ni and Mo species blocked some pores in the alumina–meso support.

Fig. 3 shows the normalized UV–vis spectra of NiMo–alumina and NiMo–alumina/meso catalysts. Seven bands were observed in the spectra of NiMo–alumina and NiMo–alumina/meso catalysts with a maximum at 15 970, 16 860, 24 130, 33 480, 36 230, 40 270 and 46 750 cm^{-1}. The identification of the individual bands to the corresponding types of Ni and Mo species was based on the literature. The doublet at 15,970–16,860 cm^{-1} and the shoulder at 24,130 cm^{-1} was attributed to the transition characteristic for tetrahedral Ni^{II}(Td) ions [11–14] and the octahedral Ni^{II}(Oh) ions [11,12,15], respectively. The bands at 33 480 cm^{-1} and 36 230 cm^{-1} were characteristic for Mo^{VI}(Oh) and Mo^{VI}(Td) species, respectively [16–19]. Unfortunately, the bands above 30,000 cm^{-1} characteristic for Mo species were also affected by Ni^{II}–O charge transfer transitions. The spectra of NiMo–alumina/meso contained slightly

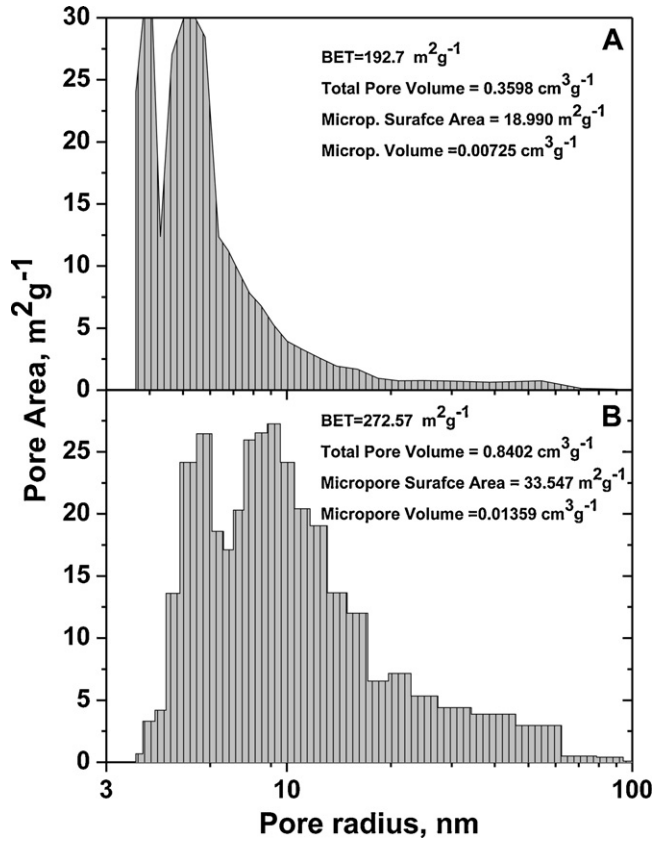

Fig. 2. Specific surfaces area, porosity and BJH pores size distribution plots of micropore surface area versus pore radius of the (A) NiMo–alumina and (B) NiMo–alumina/meso catalysts.

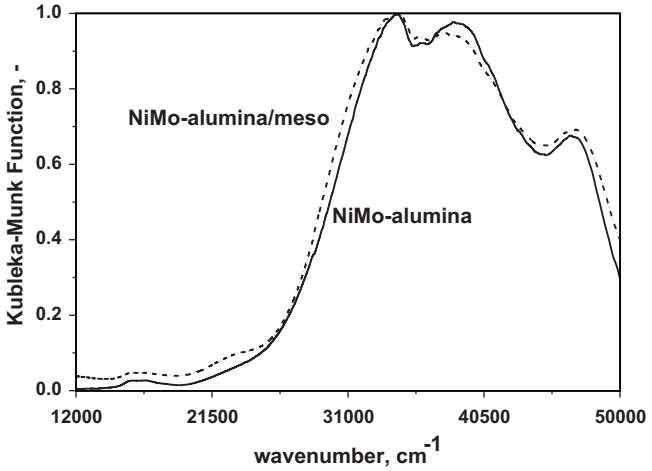

Fig. 3. Normalized UV–vis spectra of NiMo–alumina/meso (dashed-line) and NiMo–alumina (solid-line) catalysts.

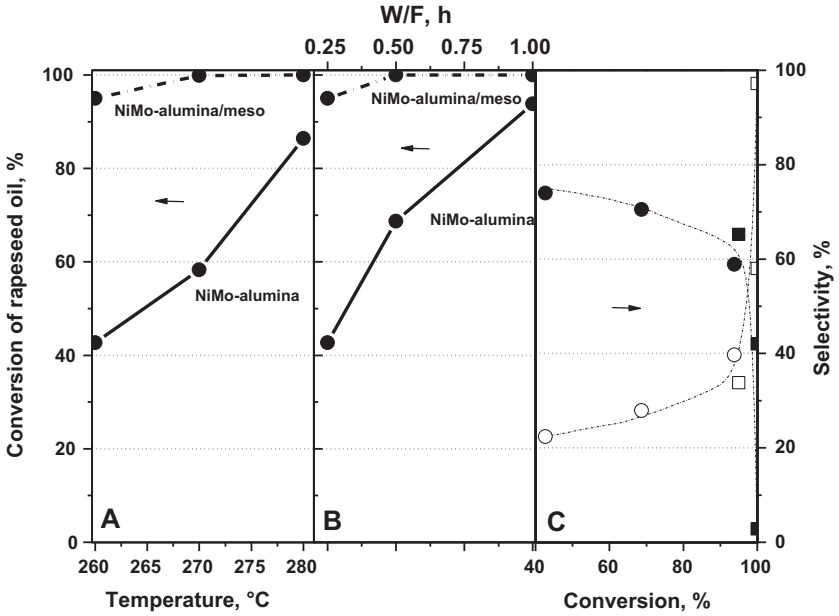

Fig. 4. (A) Dependence of the conversion of rapeseed oil on temperature in the deoxygenation of rapeseed oil at *W*/*F* 0.25 h over NiMo–alumina/meso (dashed line) and NiMo–alumina (solid line) catalysts; (B) dependence of the conversion of rapeseed oil on catalyst weight/total flow (*W*/*F*) ratio in the deoxygenation of rapeseed oil at 260 °C over NiMo–alumina/meso (dashed line) and NiMo–alumina (solid line) catalysts; and (C) dependence of the selectivity of oxygenates (solid symbols) and hydrocarbons (open symbols) as a function of the conversion of rapeseed oil at 260 °C over NiMo–alumina/meso (squares) and NiMo–alumina (circles) catalysts.

higher intensity of the bands at 24,130 cm^{-1} and 33,480 cm^{-1} representing the presence of the Ni^{II}(Oh) species and the Mo^{VI}(Oh) species, respectively, and slightly lower intensity of the band at 36,230 cm^{-1} characteristic for the Mo^{VI}(Td) species. Thus, it was concluded that the difference in the distribution of the bands characteristic for Ni and Mo species in the spectra of NiMo–alumina and NiMo–alumina/meso catalysts was insignificant, suggesting that a similar distribution of the Ni and Mo species was achieved on the alumina and alumina/meso materials.

Fig. 4A shows the dependence of the conversion of rapeseed oil on the reaction temperature in its deoxygenation over NiMo–alumina and NiMo–alumina/meso catalysts at *W*/*F* = 0.25 h. Fig. 4B shows the dependence of the conversion of rapeseed oil as a function of *W*/*F* (the ratio of catalyst mass (*W*, g) and rapeseed oil feed rate (*F*, g/h), *i.e.* contact time, in deoxygenation over NiMo–alumina and NiMo–alumina/meso catalysts at 260 °C. It is clearly seen that the conversion is higher for NiMo–alumina/meso in comparison with NiMo–alumina.

Oxygenates and hydrocarbons are the most important products of triglyceride deoxygenation. Previously, several authors suggested that the formation of oxygenates precedes that of hydrocarbons [9,20]. The selectivity-conversion behaviour (the dependence of the selectivity to oxygenates and hydrocarbons on the conversion of rapeseed oil) of NiMo–alumina/meso and NiMo–alumina catalysts was difficult to compare due to the high activity of NiMo–alumina/meso catalyst (Fig. 4C). Nevertheless, no significant difference was observed in the selectivity-conversion behaviour at around 90% conversion. To analyse the selectivity-conversion behaviour in more detail, further experiments would be needed in the future to obtain data at lower conversion levels and for more catalysts.

NiMo–alumina and NiMo–alumina/meso catalysts were prepared with the same amount of Ni (3.0 wt.%) and Mo (6.0 wt.%) and by the same preparation procedure. Moreover, the impregnation of Ni and Mo species also led to catalysts with similar distribution of metal species (Fig. 3). Thus, the main difference between NiMo–alumina/meso and NiMo–alumina catalysts was the specific surface area and the pore size distribution (Fig. 2). NiMo–alumina/meso exhibited significantly higher specific surface area and the total pore volume than the NiMo–alumina catalyst, which originated from the conventional alumina support.

On the other hand, the industrially available alumina/meso support exhibited a broad pore-size distribution (Fig. 2B), while organized mesoporous alumina could be synthesized in a laboratory with a narrow pore-size distribution [7]. Thus, it could be expected that the defined small-scale synthesis of organized mesoporous alumina could lead to a better structural properties and thus result in the further enhancement of the catalytic properties of NiMo–alumina/meso catalysts.

The NiMo–alumina and NiMo–alumina/meso exhibited relatively stable activity in the deoxygenation of rapeseed oil. The decrease in deoxygenation activity is estimated to be less than 5% during the 100 h catalytic run based on the previous results [21]. Moreover, the XRF analysis proved that the amount of Ni and Mo species in the spent catalysts was approximately the same as in the fresh ones.

It is generally accepted that the impregnation of metal species on the support with higher specific surface area leads to the higher dispersion of metal species on the support. However, only a minimum difference was observed in the distribution of Ni and Mo species in NiMo–alumina and NiMo–alumina/meso catalysts. Neither NiO- nor MoO_3-like species were present in the prepared catalysts, as evidenced from the absence of their characteristic UV–vis bands (Fig. 3) and XRD (Fig. 1) diffraction peaks.

Thus, the better performance of NiMo–alumina/meso, as evidenced by the higher conversion of rapeseed oil, was attributed to the significantly higher specific surface area and the total pore volume of NiMo–alumina/meso in comparison with the NiMo–alumina.

4. Conclusions

The NiMo–alumina/meso and NiMo–alumina catalysts were prepared using commercially available mesoporous alumina support and the conventional alumina support, respectively. The NiMo–alumina/meso catalyst showed significantly better perfor-

mance than the NiMo–alumina catalyst in the deoxygenation of rapeseed oil. As both catalysts were prepared with the same amount of Ni and Mo species, by the same procedure and they also exhibited the similar population of Ni and Mo species, the type of alumina support played the critical role in the reaction. The better deoxygenation performance of NiMo–alumina/meso could be explained by the significantly higher specific surface area and the total pore volume of NiMo–alumina/meso in comparison with the NiMo–alumina.

Acknowledgments

The authors gratefully thank the Ministry of Industry and Trade of the Czech Republic (project FT-TA3/074) and Ministry of Education, Youth and Sports (No. MSM0021627501).

References

[1] I. Kubičková, D. Kubička, Waste Biomass Valor., in press, doi:10.1007/s12649-010r-r9032-8.
[2] J. Gusmão, D. Brodzki, G. Djega-Mariadassou, R. Frety, Catal. Today 5 (1989) 533–544.
[3] I. Sebos, A. Matsoukas, V. Apostolopoulos, N. Papayannakos, Fuel 88 (2009) 145–149.
[4] J. Walendziewski, M. Stolarski, R. Luzny, B. Klimek, Fuel Process. Technol. 90 (2009) 686–691.
[5] D. Kubička, L. Kaluža, Appl. Catal. A 372 (2010) 199–208.
[6] P. Šimáček, D. Kubička, G. Šebor, M. Pospíšil, Fuel 88 (2009) 456–460.
[7] J. Čejka, Appl. Catal. A 254 (2003) 327–338.
[8] A. Taguchi, F. Schüth, Microporous Mesoporous Mater. 77 (2005) 1–45.
[9] D. Kubička, P. Šimáček, Žilková.F N., Top. Catal. 52 (2009) 161–168.
[10] J. Sanchez-Valente, X. Bokhimi, J.A. Toledo, Appl. Catal. A 264 (2004) 175–181.
[11] D. Nikolova, R. Edreva-Kardjieva, M. Giurginca, A. Meghea, J. Vakros, G.A. Voyiatzis, Ch. Kordulis, Vib. Spectrosc. 44 (2007) 343–350.
[12] M.A. Zanjanchi, A. Ebrahimian, J. Mol. Struct. 693 (2004) 211–216.
[13] Ch. Lepetit, M. Che, J. Phys. Chem. 100 (1996) 3137–3143.
[14] R.A. Schoonheydt, D. Roodhooft, H. Leeman, Zeolites 7 (1987) 412–417.
[15] L. Yang, K. Xia, Solid State Commun. 90 (1994) 737–739.
[16] A. Guevara-Lara, R. Bacaud, M. Vrinat, Appl. Catal. A 328 (2007) 99–108.
[17] H. Jeziorowski, H. Knoezinger, J. Phys. Chem. 83 (1979) 1166–1173.
[18] Y.V. Plyuto, I.V. Babich, I.V. Plyuto, A.D. Van Langeveld, J.A. Moulijn, Colloids Surf., A 125 (1997) 225–230.
[19] G.M.S. El Shafei, N.A. Moussa, Ch.A. Philip, J. Colloid Interface Sci. 228 (2000) 105–113.
[20] G.W. Huber, P. O'Connor, A. Corma, Appl. Catal. A 329 (2007) 120–129.
[21] D. Kubička, J. Horáček, Appl. Catal. A, doi:10.1016/j.apcata.2010.10.034, in press.